

## Preparation, Characterization and Gas Sensing Performance of Pure SnO<sub>2</sub> Thin Films Deposited using Physical Vapour Deposition Technique

**K. S.Thakare<sup>1</sup>, S. J. Patil<sup>3</sup>, S. B. Deshmukh<sup>2</sup>, R. Y. Borse<sup>2</sup>, R. R. Ahire<sup>1</sup>**

<sup>1</sup>S.G.Patil Arts, Science and Commerce College, Sakri, Dist- Dhule (MS) India.

<sup>2</sup>Thin and Thick Film Research Lab, M. S. G. Arts, Science and Commerce College, Malegaon-Camp, Dist- Nashik (MS) India.

<sup>3</sup>Department of Physics, L.V.H. College, Nashik (MS) India.

---

**Type of Review :** Peer Reviewed.

DOI: <http://dx.doi.org/10.21013/jte.v4.n2.p2>

### How to cite this paper:

**Thakare, K., Patil, S., Deshmukh, S., Borse, R., & Ahire, R.** (2016). Preparation, Characterization and Gas Sensing Performance of Pure SnO<sub>2</sub> Thin Films Deposited using Physical Vapour Deposition Technique. *IRA-International Journal of Technology & Engineering* (ISSN 2455-4480), 4(2), 103-116. doi:<http://dx.doi.org/10.21013/jte.v4.n2.p2>

---

© Institute of Research Advances



This work is licensed under a [Creative Commons Attribution-Non Commercial 4.0 International License](https://creativecommons.org/licenses/by-nc/4.0/) subject to proper citation to the publication source of the work.

**Disclaimer:** The scholarly papers as reviewed and published by the Institute of Research Advances (IRA) are the views and opinions of their respective authors and are not the views or opinions of the IRA. The IRA disclaims of any harm or loss caused due to the published content to any party.

---

**ABSTRACT**

*Nanocrystalline SnO<sub>2</sub> thin films were successfully prepared using Physical Vapour Deposition technique and were annealed at 400°C. Structural, morphological, elemental, compositional, optical, and electrical and gas sensing properties were studied using XRD, FESEM, EDXS, UV-Vis Spectrophotometer, DC resistance measurement method respectively. Acetone, Cl<sub>2</sub>, CO<sub>2</sub>, Ethanol, H<sub>2</sub>S and NH<sub>3</sub> sensing performance of Nanocrystalline physically vaporized SnO<sub>2</sub> thin films were investigated and reported in this paper. The results were systematically tabulated, interpreted and discussed.*

**Keywords:** SnO<sub>2</sub> thin film, PVD technique, XRD, FESEM, gas sensor, sensitivity.

**Introduction**

Since last few decades there has been an increasing interest to prepare inexpensive SnO<sub>2</sub> thin films. Tin oxide is the most widely used metal oxide semiconductor in gas sensing because of its capability to detect combustible and hazardous gases such as methane, LPG, CNG, CO, CO<sub>2</sub>, Cl<sub>2</sub>, H<sub>2</sub>S etc [1-4]. It is an n-type semiconductor of tetragonal structure with band gap energy about 3.6 eV at room temperature. It is cheap, nontoxic and has strong oxidizing power, high photochemical corrosive resistance, good electrical, optical and piezoelectric behavior. In recent years, semiconductor metal oxide films have received considerable attention because of their potential applications [5] such as photochemical and photoconductive devices in LCD, lithium-ion batteries, [6-8] a transport conductive electrode for solar cells [9,10] a gas sensing material for gas sensor devices [11], transport conducting electrodes [12] etc. The majority of the applications adopted SnO<sub>2</sub> as the sensing material due to its high sensitivity and stability at lower operational temperatures, in spite of its poor selectivity [13]. Out of many thin film preparation techniques such as chemical vapour deposition [14], spray pyrolysis [15], sputtering [16], activated reactive evaporation [17], etc. Physical Vapour Deposition method is straight forward and simple one. Because of deposition in high vacuum and at room temperature, this technique produces contamination free uniform thin films. In the present study, we used Hind Hivac vacuum depositing unit for depositing pure tin onto the cleaned glass substrates at room temperature. The films were then heated in muffle furnace at 200°C for 24 hrs to allow oxidation. The so formed pure SnO<sub>2</sub> thin films were then annealed at 300, 400 and 500°C each for 2 hrs. Structural, morphological, electrical, optical and gas sensing characterizations of the samples were studied.

**2. Experimental****2.1 Substrate Cleaning**

Glass substrates were thoroughly cleaned by hot chromic acid to remove contamination. They were then rinsed with distilled water followed by acetone. Finally the substrates were dried under UV lamp at 60-80°C.

**2.2 Preparation of nanocrystalline SnO<sub>2</sub> thin films**

Pure SnO<sub>2</sub> thin films were deposited onto the glass substrates by thermal evaporation technique. The cleaned substrates were mounted onto the mask placed ~15 cm above the tungsten basket. In this method, tin was vaporized by passing appropriate current through spiral of basket using dimmerstat (0-10 A). The selection of a particular heater depends upon the form of the material to be evaporated. When the material is heated in vacuum (~10<sup>-5</sup> mbar), it undergoes sublimation and atoms get transported to the substrates where they get deposited. The samples were then placed in a muffle furnace for 24 hrs at 200°C for allowing oxidation. Out of oxidized samples, a few samples were annealed at 400°C for 2 hrs.

### 3. Results and Discussion

#### 3.1 Electrical Characterization

##### 3.1.1 I-V Characteristics

Simple series circuit of the sample and picoammeter with voltmeter in parallel was used to study I-V characteristics. The current versus voltage characteristics of the samples annealed at 400°C were plotted. They are almost symmetrical in nature and prepared samples are ohmic in nature. The resistance values were obtained from the slope of the graphs (Fig.1).

##### 3.1.2 Resistance versus Temperature Characteristics

The electrical properties of the samples were studied. DC resistance measurement of the films was performed by using the voltage divider consisting of a standard high resistor in series with sample and a standard voltage source. Voltage across the standard resistor was measured at different temperatures (ranging from 400°C to 50°C) and film resistance was calculated. The film resistance  $R$  ( $\Omega$ ) was plotted against temperature  $t$  ( $^{\circ}\text{C}$ ) (Fig. 2a) and temperature coefficient of resistance (TCR) of the film material was calculated. Graph showed negative temperature coefficient of resistance and semiconducting nature of the samples.

Graph of  $\log R$  versus  $1/T$  ( $T$  being sample temperature in  $\text{K}$ ) (Fig.2b) was used to evaluate activation energy in high and low temperature regions. The results are tabulated in Table1. The activation energy of tin oxide films is due to the formation of donor levels below conduction band. Earlier researchers have obtained activation energy to be 0.26 eV and 0.2 eV [18]. Some other groups reported activation energy as 0.73 eV [19].

#### 3.2 Structural Characterization by XRD

The crystalline structure of the thin films was examined by X-Ray Diffractometer (Model-D8 Advance, Make-Bruker AXS GmbH, Berlin, Germany) using  $\text{CuK}\alpha$  radiation having wavelength 1.5402  $\text{A}^{\circ}$  within  $2\theta$  range of  $20^{\circ}$  to  $80^{\circ}$ . Fig.3 shows the XRD patterns of the samples annealed at 400°C. All the major peaks correspond to tetragonal phase. Open peaks correspond to the substrate (glass) material. Average Crystallite size was estimated using Scherrer formula.

$$D = \frac{0.9\lambda}{\beta \cos\theta} \quad \text{----- (1)}$$

where,  $D$  is crystallite size,  $\lambda$  is wavelength of radiation (1.5402  $\text{A}^{\circ}$ ),  $\beta$  is Full Width at Half Maxima in radians and  $\theta$  is Bragg's angle in degrees.

Interplanar distance  $d$  was determined using Bragg's condition  $2d \sin \theta = n \lambda$ . Degree of crystallinity [19], grain size, interplanar distance, average texture coefficient, dislocation density, lattice strain etc. were also determined using the relations (eq.1-7) [20-22] and systematically tabulated in Table 2.

$$d = \frac{\lambda}{2 \sin\theta} \quad \text{----- (2)}$$

$$\text{Dislocation density} = \frac{1}{D^2} \quad \text{----- (3)}$$

$$\text{D. C.} = \frac{I_c}{I_c + I_a} \quad \text{----- (4)}$$

$$g = \frac{\beta}{\tan\theta} \quad \text{----- (5)}$$

$$S. A. = \frac{6}{\rho D} \quad \text{----- (6)}$$

$$\text{Texture Coefficient } t = \frac{I/I_0}{\frac{1}{N} \sum \frac{1}{I_0}} \quad \text{----- (7)}$$

where I = the measured intensity, I<sub>0</sub>= the standard intensity, N = number of diffraction peaks, I<sub>c</sub> and I<sub>a</sub> are respectively the intensities corresponding to crystalline and amorphous phases, ρ = density of the material in g/cc. The observed grain size from XRD patterns and FE-SEM were estimated, their values were compared.

All these structural parameters have been determined and reported in Table 2. Since the averaged texture coefficient value was 1 the formed material in thin films is confirmed to be polycrystalline in nature. The corresponding (hkl) planes for 2θ values matched with standard JCPDS data cards [23].

### 3.3 Surface Morphology by FESEM

The surface morphology of the films were observed using FESEM technique (Model-S4800 Type II, Make-Hitachi HiTechnologies Corporation, Tokyo, Japan).

Fig. 4 shows the FESEM micrograph images of pure SnO<sub>2</sub> thin film samples annealed at 400°C. The small spherical grains residing on some large, irregular shaped grains were observed from FESEM image. Micrograph shows that the grains are nano-crystalline in nature. Average grain size was estimated to be 140 nm which is much larger than 14.13 nm, the crystallite size obtained from XRD. It is found that films have uniform and smooth morphology having nanocrystalline nature with optical porosity. Optical porosity is advantageous for gas sensing. [24].

### 3.4 Elemental Composition: EDXS

Elemental composition of the films was determined by EDXS (Model-XFLASH5030 Detector, Make-Bruker Nano GmbH, Berlin, Germany). The EDXS spectrograph for SnO<sub>2</sub> thin film samples annealed at 400°C is presented in fig. 5

Stoichiometrically expected at. % of Sn and that of O are 33.3 and 66.7 respectively. Observed at. % of Sn and O were as shown in the table above. They are much deviated from the expected values. Nevertheless, the prepared SnO<sub>2</sub> polycrystalline films are nonstoichiometric in nature and it is beneficial for gas sensing.

### 4. Optical Parameters by UV-Vis spectrophotometer

Fig.6 shows the absorbance of tin oxide thin film. Optical characterization of tin oxide films offers information about physical properties such as band gap energy, band structure and optically active defects etc. [25]. To obtain band gap, absorption coefficient was calculated from absorption data. Fig. 6 graph of (α) versus (λ). Band gap was then calculated by plotting (α hν)<sup>2</sup> versus (hν) using the equation

$$\alpha h \nu = A(h \nu - E_g)^n$$

where α is absorption coefficient, A is a constant, E<sub>g</sub> is the optical band gap energy, hν is the photon energy and n is constant. Value of n can be 1/2 or 2 depending upon the presence of the allowed direct and indirect transitions [25]. Fig. 7 shows graph of (α hν)<sup>2</sup> versus (hν). Nature of the plot suggests direct interband transitions.

Band gap is determined by drawing tangent to the curve near the energy axis. The point where the line intersects the axis gives the band gap value. It is observed to be about 3.8 eV.

## **5. Gas Sensing Properties**

### **5.1 Details of the Static Gas Sensing System**

The static system for examining the performance of test gases is shown in fig.8. It consists of a glass chamber of known volume which encloses the sample, a Cr-Al thermocouple and electrical heater. They were connected to various ports fitted to base plate of the system. These ports enabled external electrical connections to voltmeter, temperature controller and dimmerstat. A known amount of a test gas was injected in the chamber through a gas inlet port using a micro syringe. The sample was heated by electrical heater by passing current monitored through dimmerstat. The thermocouple output was given to temperature indicator to know the sample temperature. A constant DC voltage was applied to the sample and voltage across a standard resistor was measured by digital voltmeter. The voltage was recorded corresponding to fixed temperature intervals. After every cycle of readings, the chamber was removed to expose the sample to air.

**Sensitivity:** Sensitivity is defined as  $S = R_a/R_g$  where,  $R_a$  is the resistance of the sample in dry air and  $R_g$  is that in the presence of a test gas measured at respective temperatures. It reveals from the graphs that the gas response increases with working temperature, reaches maximum at particular temperature (operating temperature) and then decreases. It is observed that gas responses are different for different gases and vary with gas concentrations of the same gas too. It reveals that operating temperatures also vary with different gases. The observations are depicted in Table 4.

**Selectivity:** The selectivity or specificity of a sensor towards an analyzing gas is expressed in terms of dimension that compares the concentration of the corresponding interfering gas that produces the same sensor signal. The selectivity profile of different gases for various gas concentrations is depicted in the fig.10 below. Out of the tried test gases, ethanol showed maximum response for 2cc concentration at an operating temperature 200°C.

## **6. Conclusions**

- The pure SnO<sub>2</sub> thin solid films were prepared by physical vapour deposition technique in vacuum of about 10<sup>-5</sup> mbar at room temperature and their various parameters were studied.
- The so prepared pure tin oxide thin films were annealed at 400°C.
- The structural and morphological properties of the prepared thin films were characterized by XRD, FESEM and EDXS. The crystallite size, average texture coefficient and grain sizes were calculated along with elemental composition of the samples.
- The band gap values were obtained from the absorption spectra and found to be about 3.8eV.
- Gas responses were obtained for different test gases. Maximum response was seen for 2cc ethanol at an operating temperature 300°C.
- The samples show good sensitivity but poor selectivity. All above observations infer that pure tin oxide thin solid films prove to be good sensing material.

## **5. Acknowledgment**

The authors are thankful to the Principal, S.G. Patil College, Sakri, Dist-Dhule and the Principal, M.S.G. College, Malegaon, Dist- Nashik for providing the laboratory facilities. The authors are also thankful to the Management authorities of S.G. Patil College, Sakri and M.G. Vidyamnadir for their constant support.

## **7. References**

- [1] J. G. Duh, J. W. Jou, B. S. Choi; J.Electrochem. Soc., 1989, 136, 27-40.
- [2] A. RatnaPhani, S. Manorama, V. J. Rao; Appl. Phys. Lett., 1995, 66,34-89.
- [3] D. S. Vlachos, C. A. Papadopoulos, J. N. Avarisiotis; Appl. Phys. Lett., 1996,69, 650.
- [4] M. Fleischer, S. Kornely, T. Weh, J. Frank, J. Meixner;Sens. Actuators B 2000,69, 205.
- [5] R. H. Bari, S. B. Patil, A. R. Bari-Synthesis, Characterization and Gas Sensing Performance of Sol-gel Prepared Nanocrystalline SnO<sub>2</sub> Thin Films, International Journal on Smart Sensing and Intelligent

- Systems, 2014, 7, 2, 610-628.
- [6] S. B. Deshmukh, R. H. Bari, G. E. Patil, D. D. Kajale, G. H. Jain, L. A. Patil, Preparation and Characterization of Zirconia based Thick Film Resistor as a Ammonia Gas Sensor, International Journal on Smart Sensing and Intelligent Systems, 2012, 5,3, 540-558.
- [7] S. Chappel, A. Zaban, Nanoporous SnO<sub>2</sub> Electrodes for Dye-sensitized Solar cells: Improved Cell Performance by the Synthesis of 18nm Colloids, Solar Energy Materials a Solar Cells, 2002, 71, 141-152.
- [8] S. Gnanam, V. Rajendram, Luminescence Properties of EG-assisted SnO<sub>2</sub> Nanoparticles by Sol-gel Process, Digest Journal of Nanomaterials and Biostructures, 2010, 5, 699-704.
- [9] Aoki A and Sasakura H J.; Appl. Phys. 1970,9,582.
- [10] Mohammadi M, Solemani E and Mansorhaseini M Mater. Res. Bull. 2005, 40, 1303.
- [11] Keshavraja A, Ramaswami A V and Vijayamohanan K Sensor Actuator B 1995,23,75.
- [12] Fukano T and Motohiro T; Sol. Energy Mater. Sol. Cells 2004,82, 567.
- [13] Hagen W, Lambrich R E and Jagois; J Adv. Solid State Phys., 1983,23,259.
- [14] T. Okuno, T. Oshima, S. Dong Lee, S. Fujita, - Growth of SnO<sub>2</sub> crystalline thin films by mist chemical vapour deposition method, Physica status solidi (c), 2011 , 8, 540-542.
- [15] K. Murakami, K. Nakajima, S. Kaneko, - Initial growth of SnO<sub>2</sub> crystalline thin films on the glass substrate deposited by the spray pyrolysis technique, Thin Solid Films, 2007 ,515, 8632-8636.
- [16] T. gui, L. Hao, J. Wang, L. Yuan, W. Jai, X. Dong-Structure and Features of SnO<sub>2</sub> Thin Films prepared by RF Reactive Sputtering, Chinese Optic Letters, 2010, 8, 10134-03,
- [17] H. S. Randhawa, M. D. Matthews, R. F. Bunshah, SnO<sub>2</sub> films by activated reactive evaporation, Thin Solid Films, 1981, 83, 267-271,
- [18] D. Das and R. Banerjee; Thin Solid Films, 1987, 147, 321.
- [19] R. Sanjines, V. Demarne and F. Levy, Thin Solid Films, 1990, 193, 935.
- [20] S. Chattopadhyay, T.C. Chaki, A.K. Bhowmick, Structural Characterization of Electron-beam Cross Linked Thermoplastic Elastomeric Films from Blends of Polyethylene and Ethylene-vinyl acetate Copolymers, J. Appl. Polym. Sci., 2001,81, 1936-1950.
- [21] B. D. Cullity, Elements of X-ray diffraction, Addison-Wesley Publishing Co., 1956.
- [22] L. E. Alexander, X-ray diffraction methods in polymer science, Wiley International, New York, 1980.
- [23] JCPDS data card of SnO<sub>2</sub> (01-072-1012 and 00-006-0395).
- [24] Patil P S, Kawa R K, Sadale S B and Chigare P S Thin Films, 2003, 34437.
- [25] G.E.Patil, D.D. Kajale, S.D. Shinde, R.H. Bari, D. N. Chavan, V.B. Gaikwad, G. H. Jain, Sensors and Transducers Journal, Vol.9, Special Issue, Dec. 2010, 96-108.

(Tables & Figures)

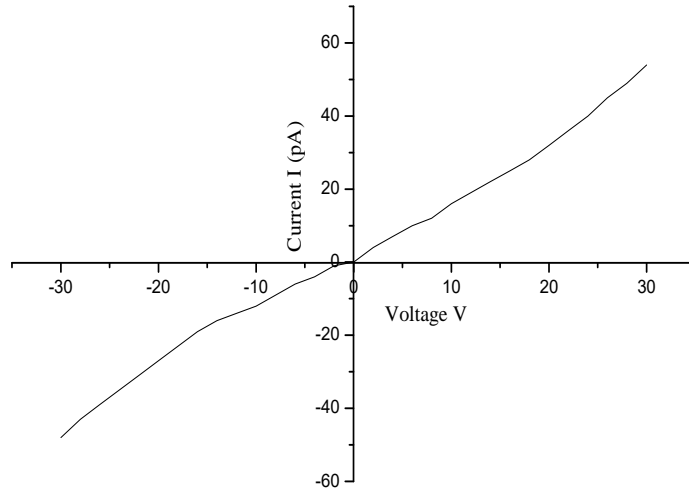


Fig. 1 I-V characteristics of SnO<sub>2</sub> thin films

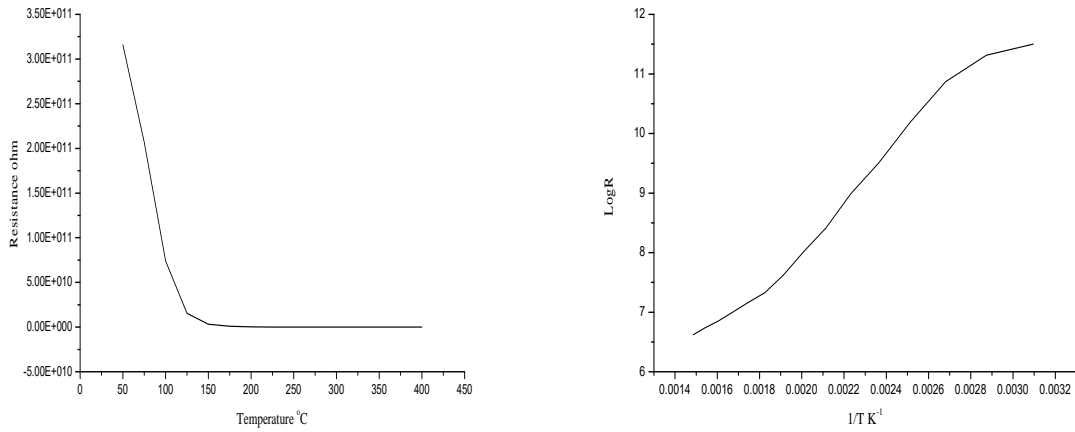


Fig. 2 Electrical Properties.

Graph of (a) Resistance R versus temperature (°C) (b) logR versus 1/T (K<sup>-1</sup>)

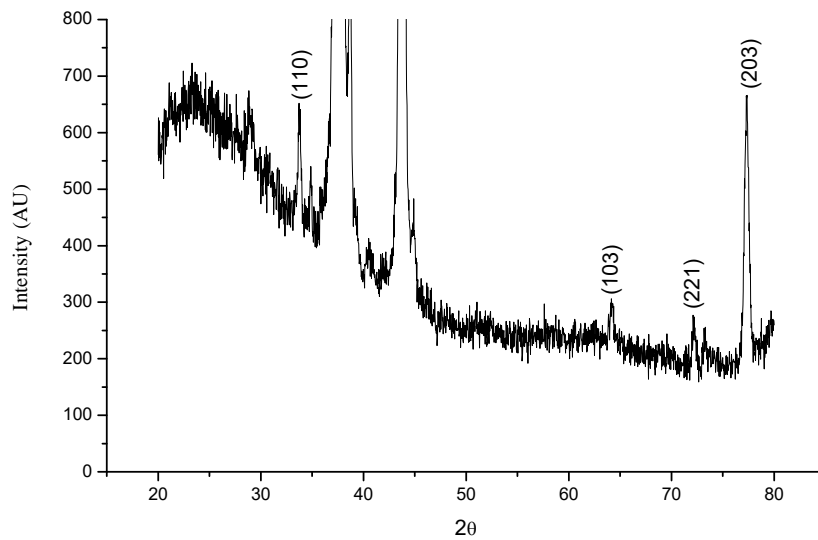


Fig. 3 XRD patterns of samples annealed at 400°C

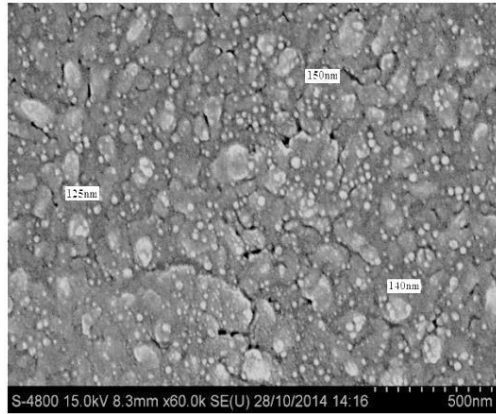


Fig. 4: FESEM micrographs of samples annealed at 400°C

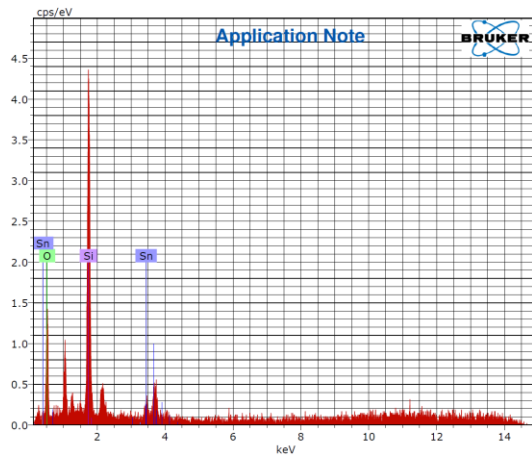


Fig. 5 Elemental analysis of samples annealed at 400°C

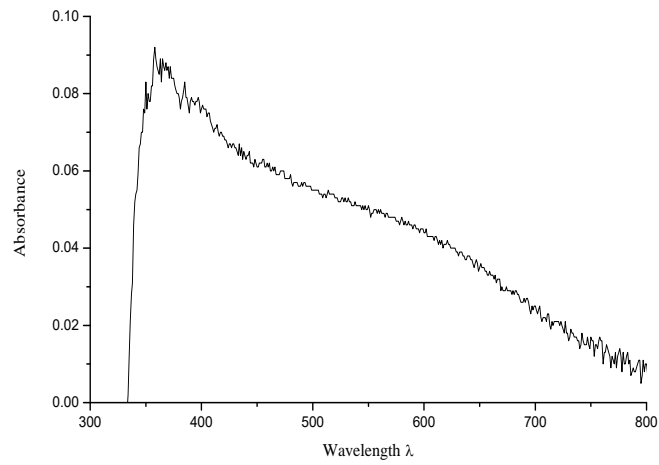


Fig. 6 Plot of absorbance versus wavelength

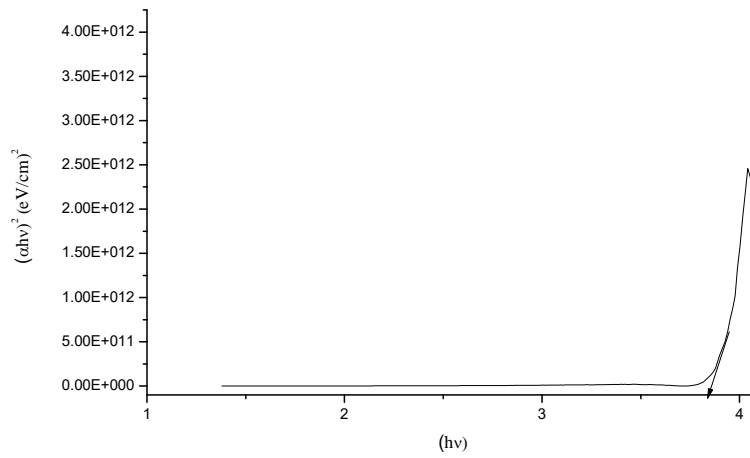


Fig. 7 graph of  $(\alpha h\nu)^2$  versus  $(h\nu)$

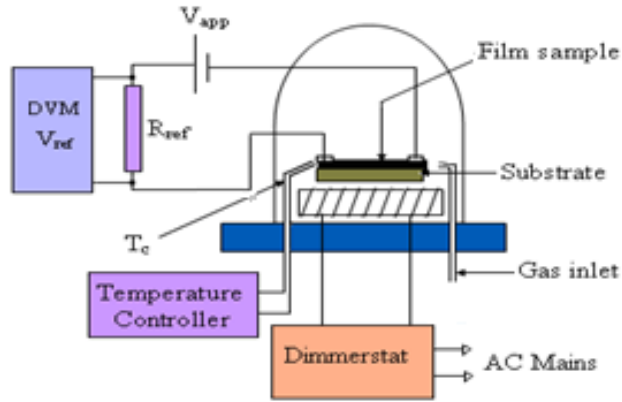


Fig.8 Static Gas Sensing System

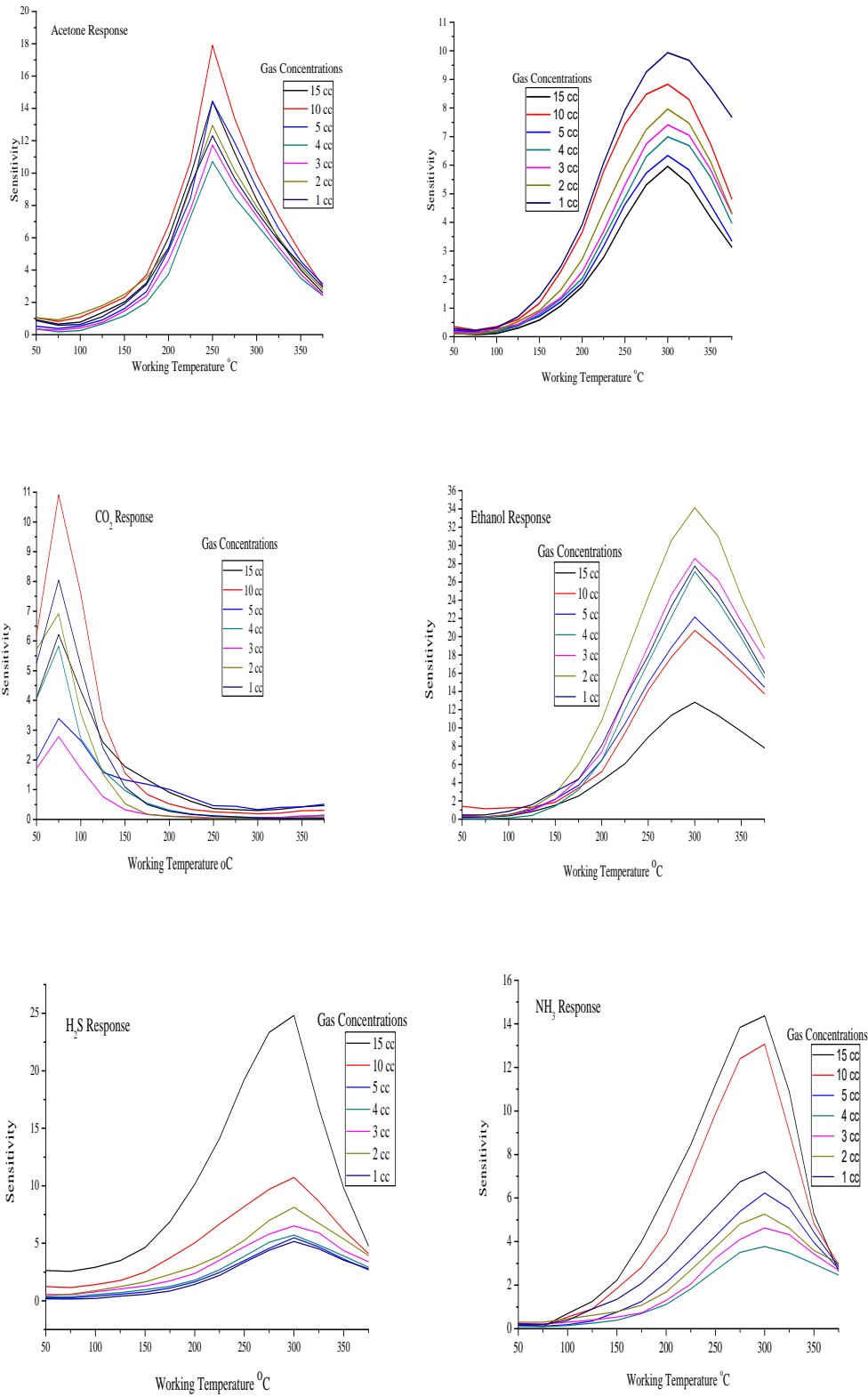


Fig. 9 SnO<sub>2</sub> thin film Sensitivity for various target gases

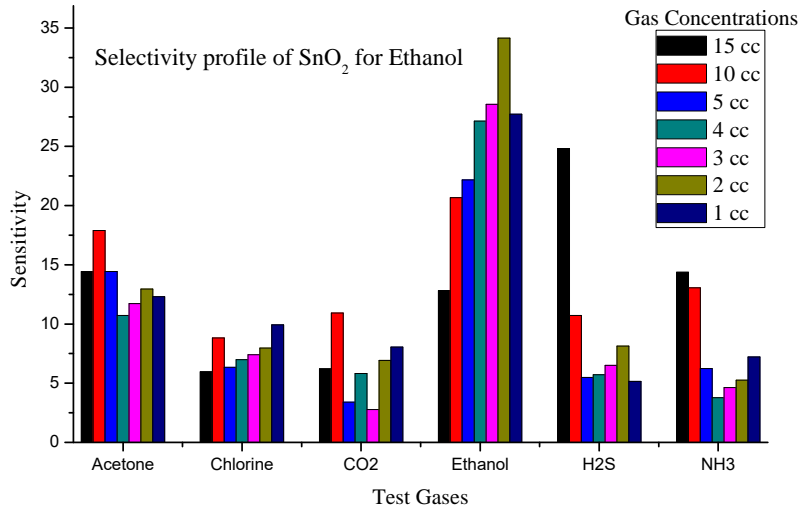


Fig.10 The selectivity profile of SnO<sub>2</sub> for ethanol

Table1

Annealing temperature °C	Resistance MΩ	TCR /°C	Activation Energy eV	
			HTR	LTR
400	6.373	-0.0019	0.411	0.850

Table 2

Annealing Temp. °C	h,k,l	2θ	Dislocation density x10 <sup>15</sup> /m <sup>2</sup>	Crystallite Size from XRD nm	Grain Size (FESEM) (nm)	Average Texture Coefficient	Lattice Strain g(%)	Interplanar Distance d A°	DC (%)
400	102	44.39	0.0050	14.13	145	1.00	0.874	2.038	70.60

Table 3

Elements	Annealing temp. 400°C	
	Mass %	At. Wt.%
O	49.10	64.73
Si	45.75	34.36
Sn	5.14	0.91
Total	100.00	100.00

Table 4

Gas	Gas Concentrations							Operating Temp °C
	15 cc	10 cc	5 cc	4 cc	3 cc	2 cc	1 cc	
Acetone	14.4362	<b>17.9020</b>	14.4362	10.7155	11.7303	12.9479	12.3101	250
Chlorine	5.9602	8.8318	6.3404	6.9904	7.4134	7.9641	<b>9.9377</b>	300
CO <sub>2</sub>	6.2199	<b>10.9213</b>	3.39194	5.8282	2.783	6.9162	8.0478	75
Ethanol	12.8197	20.6769	22.1651	27.1342	28.5608	<b>34.1464</b>	27.7286	300
H <sub>2</sub> S	<b>24.816</b>	10.7240	5.4777	5.7108	6.5156	8.1343	5.1554	300
NH <sub>3</sub>	<b>14.3698</b>	13.0648	6.2278	3.78	4.6281	5.2595	7.2143	300